ELSEVIER

Chemical Geology 173 (2001) 193–205

CHEMICAL GEOLOGY
INCLUDING
ISOTOPE GEOSCIENCE

www.elsevier.com/locate/chemgeo

Methane-bearing aqueous fluid inclusions: Raman analysis, thermodynamic modelling and application to petroleum basins

Jean Dubessy [a,*], Stéphane Buschaert [a], William Lamb [b], Jacques Pironon [a], Régis Thiéry [a,1]

[a] *UMR 7566, Géologie et Gestion des Ressources Minérales et Energétiques, CREGU, Université Henri Poincaré, BP-239, 54506-Vandœuvre-lès-Nancy Cedex, France*

[b] *Department of Geology and Geophysics, Texas A and M University, TX USA*

Accepted 18 January 2000

Abstract

Calibration for the determination of the CH_4/H_2O ratio using Raman spectroscopy is carried out using synthetic fluid inclusions with 0 m NaCl. Spectra of the symmetric stretching band of methane (ν_{1,CH_4}), and the bending (ν_{2,H_2O}) and stretching (ν_{S,H_2O}) bands of water were obtained in the aqueous phase co-existing with the vapour phase at variable temperatures from 25° to a few degrees above the homogenisation temperature. A software program, based on the model of Duan et al. (1992a) [Duan, Z., Moller, N., Greenberg, J.H., Weare, J.H. 1992a. The prediction of methane solubility in natural waters to high ionic strength from 0°C to 250°C and from 0 to 1600 bar. Geochim. Cosmochim. Acta, 56, 1451–1460.] has been developed to calculate the composition of the aqueous liquid phase co-existing with the vapour phase in the synthetic fluid inclusions. Application to natural samples from the Alwyn South area (North Sea) shows that Raman analyses permit discrimination between inclusion populations that are not recognised using only microthermometric measurements. These results provide important constraints on the P–T conditions of inclusion formation and suggest that oil migration occurred at fluid pressures of approximately 240 bars. © 2001 Elsevier Science B.V. All rights reserved.

Keywords: System H_2O–CH_4; Fluid inclusions; Raman analysis; Isochore; Thermodynamic modelling; Oil sedimentary basins

1. Introduction

The reconstitution of the pressure–temperature (P–T)-time path is a key parameter for the evaluation of the oil potential of a sedimentary basin. Fluid inclusions, which have trapped palaeo-diagenetic fluids, may be a powerful tool for the reconstruction of the P–T conditions, provided the molar volume and composition of the inclusions are correctly determined.

Methane is always a component of the oil phase in the oil window and could eventually form a separate vapour phase (Gravier, 1986). Consequently, methane is also dissolved in the aqueous phase co-existing with the hydrocarbon-rich phase and represents the dominant hydrocarbon component because hydrocarbons, heavier than methane, are much less soluble (Price, 1981).

* Corresponding author.
E-mail address: jean.dubessy@g2r.u-nancy.fr (J. Dubessy).
[1] Present address: Département des Sciences de la Terre, Université Blaise Pascal, 2-5, rue Kessler, 63038-Clermont-Ferrand-Cedex, France.

0009-2541/01/$ - see front matter © 2001 Elsevier Science B.V. All rights reserved.
PII: S0009-2541(00)00275-8

The concentration of methane in aqueous solutions at sedimentary P–T conditions is always small, typically below 0.2 m, and its identification in fluid inclusions is difficult. Methane in fluid inclusions can be identified using microthermometry, either by a liquid–vapour phase transition ($L + V \rightarrow V$) occurring in the non-aqueous part of the inclusion below the critical point of methane (-82.4°C) or by clathrate formation and dissolution. Calculation of the limit of detection of methane contained in a fluid inclusion can be approximated given the volume of the methane-rich vapour bubble at room temperature, and assuming that the density of the aqueous phase is 1 g cm^{-3}. For example, if the methane vapour phase occupies 10 vol.% of a spherical inclusion that has a radius of 11 μm, then the limit of detection is 0.9 m at a temperature of at least -170°C. This determination is based on the resolving power of an optical microscope (around 0.7 μm), and assumes a methane phase of critical density. Methane in aqueous fluid inclusions may also be detected by the presence of clathrates with elevated melting temperatures. The presence of methane-bearing clathrates requires a pressure higher than that of the "Q" point (27 bar at 0°C in a salt-free system, Deaton and Frost (1948)), and indicates methane concentrations must be at least 0.06 m. However, the presence of salts, which destabilise the clathrate, and the difficulty of identification of clathrate suggest a limit of detection around 0.1 m. Consequently, microthermometric measurements do not allow the identification of methane in aqueous fluids typical of sedimentary basins.

Fluid inclusions may be used to constrain P–T conditions of inclusion formation only if an isopleth can be accurately projected in P–T space. The projection of isopleths in the P–T plane depends on the concentrations of CH_4 and salt (e.g. NaCl) in the fluid inclusion. For example, at 100°C, a 0.1 m CH_4 aqueous solution has a bubble pressure of about 150 bar, according to the model of Duan et al. (1992a), a value much higher than the 1-bar fluid pressure of the H_2O–NaCl system with the same salinity (Fig. 1). Furthermore, pressure increases to 200 bar if the NaCl concentration increases to 1 m, and to 800 bar if the NaCl concentration is 4m. Therefore, failure to detect methane by microthermometry may lead to a misinterpretation of fluid inclusion data by an underestimation of fluid pressure or overestimation of fluid temperature. The aim of this paper is to calibrate the Raman microprobe for the analysis of CH_4 at low concentration ($0.01 < m\ CH_4 < 2$m) in fluid inclusions of the H_2O–CH_4 system, and to apply this technique to the analysis of methane in natural systems with fluids of low-salinity.

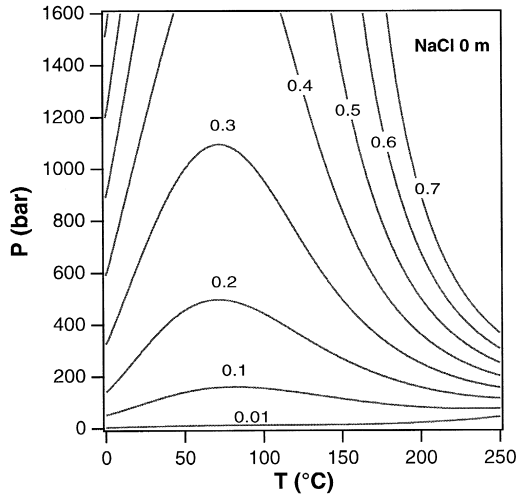

Fig. 1. Projection of several isopleths in the P–T plane of the system H_2O–CH_4 calculated from the model of Duan et al. (1992a). The methane concentration is indicated along the L + V–> L isopleths in the molality scale.

2. Experimental procedures

Synthetic fluid inclusions have been prepared in fluorite. This mineral was chosen because thermal microcracks heal easily at temperatures as low as 200°C, which is not the case for quartz, which requires much higher temperatures (Bodnar and Sterner, 1987). To ensure fluid trapping in the single-phase field, the P–T conditions of fluid inclusion synthesis were 400°C and 5 kbar. The experimental procedure employed in inclusion synthesis has been described by Frantz et al. (1989) and Lamb et al. (1996). Analysis of the compositions of fluids present in noble metal capsules using mass spectrometry by Frantz et al. (1989), gas chromatography (Zhang and Frantz, 1987), and weight changes (Lamb et al., 1996), all indicate that fluid compositions do not change during inclusion synthesis experiments. These

observations, in conjunction with the observation that phase relations determined from synthetic inclusions are generally in excellent agreement with phase relations determined for the same systems using other, more conventional techniques (e.g. Zhang and Frantz, 1992), provide strong evidence that synthetic fluid inclusions contain representative samples of the fluid originally loaded into the capsule.

Microthermometric data were obtained using a USGS-type heating and freezing stage. This stage was calibrated using the temperature of the CO_2 triple point (-56.6°C) of natural fluid inclusions checked for the absence of other gases (< 0.1 mol%) by Raman spectroscopy. The triple point of H_2O (0°C) and the critical homogenisation of an H_2O fluid inclusion (374.1°C) were also used for the calibration. The accuracy of measurements is ± 0.1°C in the range of -100°C to $+25$°C, ± 0.5°C between 25°C and 250°C and increases linearly to ± 1°C at 374.1°C.

A ChaixMeca (®) stage fixed to the Raman spectrometer was used without its cover glass to heat the samples to the homogenisation temperature (T_h) in increments of 25°C. Calibration of the stage was

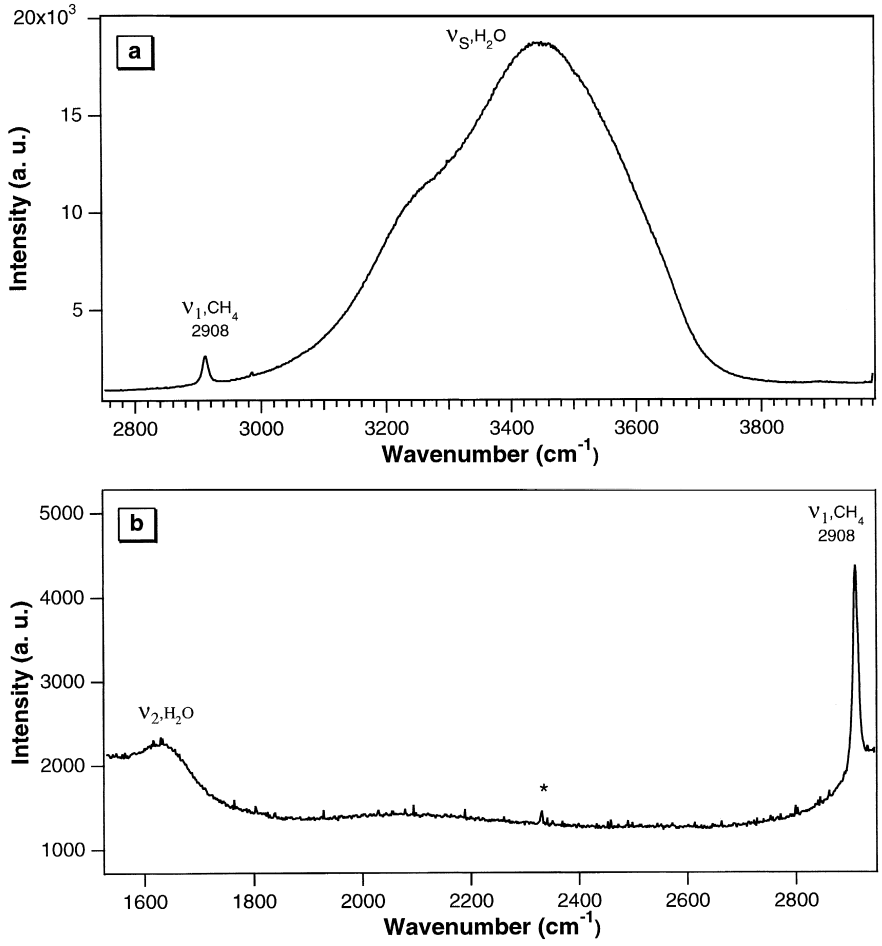

Fig. 2. (a) Raman spectra of the stretching band of water (3000–3700 cm^{-1}) and the symmetric stretching band of methane ($\nu_{1,CH_4} = 2908$ cm^{-1}). $T = 100$°C; sample 117. (b) Raman spectra of the bending mode of water (ν_2) at ~ 1640 cm^{-1} and the symmetric stretching band of methane ($\nu_{1,CH_4} = 2908$ cm^{-1}). The weak peak at 2330 cm^{-1} is the line of atmospheric nitrogen above the sample. $T = 100$°C; sample 117. *: Raman of nitrogen from the air.

made by reference to fluid inclusion homogenisation temperatures measured with the USGS stage; the accuracy is ± 1°C.

The Raman spectrometer is a Labram-type (® Dilor), equipped with a Notch (® Kaiser) filter and with only one grating (1800 grooves/mm) which results in high optical throughput. The detector is a CCD cooled at -30°C. The exciting radiation is provided by an Ar^+ laser (Type 2020, ® Spectraphysics). The spectral resolution is 2 cm^{-1}. Integration time used for the stretching band of water is 60 s with a few accumulations and 100 s with a few accumulations for the bending mode of water.

Raman spectra were collected in two spectral windows, 2700–4000 cm^{-1} (Fig. 2a) and 1500–2950 cm^{-1} (Fig. 2b). The spectral region from 2700 to 4000 cm^{-1} contains the large stretching band of water (2900–3700 cm^{-1}) and the ν_{1,CH_4} band of methane (2908 cm^{-1}) (Fig. 2a). The ν_{3,CH_4} band at 3006 cm^{-1}, the anti-symmetric stretching band and the overtones ($2\nu_4 = 2576$ cm^{-1} and $2\nu_2 = 3070$ cm^{-1}) were not identified because they are too weak. The weak bending mode of water is identifiable together with the symmetric stretching of methane (ν_{1,CH_4}).

No data processing has been used for the spectra of the stretching mode of water, recorded in the 2700–4000 cm^{-1} range. For the 1500–2950 cm^{-1} spectral range, we performed signal processing using the software of Rull et al. (1996). A fast Fourier transform filtering procedure was used to remove noise within the range 1500–2950 cm^{-1}: a medium and high frequency filter was used for the bending mode and only a medium frequency filter was used for the ν_{1,CH_4} band to prevent modifying the shape, position and width of this band shape. The Raman spectrum with the highest intensity of the ν_{1,CH_4} band was peak-fitted in order to determine its profile or the percentage of gaussian and lorentzian components. For the other spectra, the wavenumber at maximum intensity, peak heights and full width at half-maximum intensity (fwhm) of the ν_{1,CH_4} band were determined by a fitting procedure with the same band profile determined previously. The area of the fitted band was then measured. The net area of the bending and stretching bands of water were measured after the removal of noise by the Fourier transform filter without any peak-fitting procedure.

3. Results

3.1. Samples

Fluid compositions and homogenisation temperatures of studied samples are given in Table 1. The homogenisation temperatures of fluid inclusions are in the range 290°C–300°C, indicating homogeneous V–X properties. However, homogenisation temperatures around 300°C seem to be inconsistent with the conditions of trapping at 5 kbar (400°C). Indeed, a bubble-point pressure of 700 bars at the homogenisation temperature (290–300°C) would require an increase of more than 4 kbar between 300°C and 400°C.

All the analysed inclusions were first studied at low temperatures for the detection of a methane clathrate. The clathrate was never identified, but it is worth noting that the vapour bubble disappeared during the nucleation of ice. In addition, the samples were prepared by thermal cracking (Sterner and Bodnar, 1984), which likely introduces dislocations in fluorite immediately adjacent to the fractures. Fluid inclusions used for this study were never heated above their homogenisation temperature by more than a few degrees. Fluorite is known as a mineral which stretches easily (Bodnar and Bethke, 1984; Wilkins, 1986). This tendency to stretch is linked with the density of dislocations which probably develop during thermal cracking of the fluorite crystal and may also form during ice formation in the absence of vapour. Stretching of the fluid inclusions could account for the high values of the homogenisation temperatures.

In Section 3.3, which is devoted to calculation of the methane concentration in the aqueous phase, it is shown that knowledge of the bulk density of the

Table 1
Composition of fluid (X: mole fraction, and m: molality scale) used for the formation of synthetic fluid inclusions made by following the procedure of Frantz et al. (1989) and Lamb et al. (1996)

Sample	X_{H_2O}	X_{CH_4}	m_{CH_4}	T_h(L)°C
115 F	0.983	0.017	0.961	294 ± 10
117 F	0.962	0.038	2.194	297 ± 5

T_h = homogenisation temperature to the liquid phase.

fluid at the P–T conditions of trapping is not required. Bulk density is determined only by using the bulk composition and the homogenisation temperature. Therefore, a change in the density of the trapped fluid, resulting from stretching of the inclusions, has no effect on the calibration procedure.

3.2. Raman spectra

At room temperature, the ν_{1,CH_4} band of methane dissolved in the aqueous phase is weak, due to the low solubility of methane in the aqueous solution. The wavenumber of this band is 2908 cm^{-1}, a value significantly different from the value of 2917 cm^{-1} for low-density methane vapour (Herzberg, 1968). During heating to 225°C, the position of the ν_{1,CH_4} band of methane dissolved in the aqueous solution remains constant.

The bending mode (ν_{2,H_2O}) of water does not change significantly both in fwhm and in wave number with temperature. On the contrary, the stretching band of water shows a shift of its maximum intensity towards higher wave number and a decrease of its shoulder around 3200 cm^{-1}, characteristic of hydrogen breaking by thermal agitation (Ratcliffe and Irish, 1982; Frantz et al., 1993; Dubessy et al., 1998).

The reproducibility of the intensity of a given Raman band is difficult to achieve especially from fluid inclusions of small size (less than 10 μm) which are heated since it is impossible to control and reproduce with sufficient accuracy the irradiation and the geometry of light collection. The intensity ratio between the two bands (CH_4 area/H_2O area) eliminates the geometrical changes of the experimental conditions and results in a smooth trend when plotted against temperature (Fig. 3a,b).

3.3. Calculation of the methane concentration in the liquid aqueous phase

The synthetic fluid inclusions exhibit homogenisation temperatures up to 300°C, which prevents the extrapolation of the (CH_4 area/H_2O area) measured in single phase fluid inclusion just above the homogenisation temperature to temperatures between 100 and 150°C, typical of homogenisation temperatures of fluid inclusions from sedimentary basins. Therefore, it is necessary to calculate the concentration of methane dissolved in the aqueous phase, which co-exists with the vapour phase. This is performed by assuming that fluid inclusions are constant mass and density systems and by using the model of Duan et al. (1992a) for the solubility of methane in aqueous solutions. An algorithm and software program has been developed to make these calculations. The main steps of these calculations are explained with the following equations. Unit of molar volume is $cm^3\ mol^{-1}$ and of density, g cm^{-3}. Concentrations are written either in mole fraction (X_i) or in the molality scale (m_i).

At the first step, the bulk density of the fluid is calculated. No equations of state are available for calculating the molar volume of fluids of known composition in the H_2O–NaCl–CH_4 system at fixed P and T. Therefore, the molar volume of the ternary

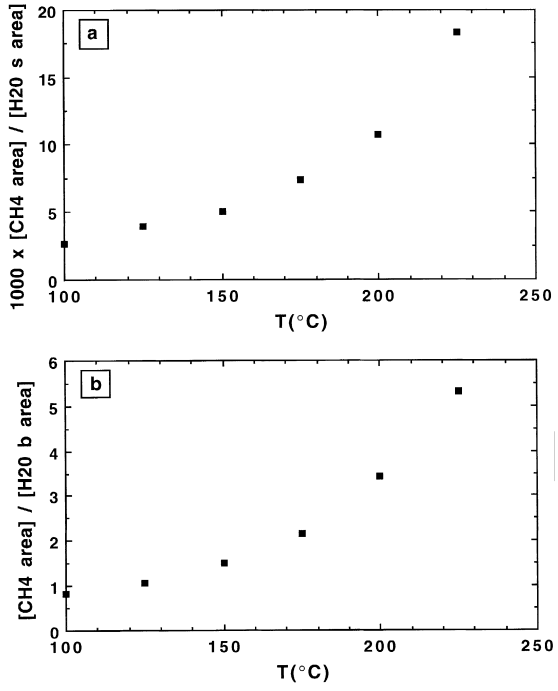

Fig. 3. (a) Variation of the ratio (CH_4 area of the ν_{1,CH_4} band)/(H_2O area of the ν_{s,H_2O} band) vs. temperature for sample 117. (b) Variation of the ratio (CH_4 area of the ν_{1,CH_4} band)/(H_2O area of the ν_{b,H_2O} band) vs. temperature for sample 117.

system was calculated by considering a pseudo-binary system with H_2O–NaCl and CH_4 as the two end-members:

$$\overline{V^{T,P}_{\mathrm{aq},m_{\mathrm{NaCl}},m_{\mathrm{CH_4}}}} \approx \left(X_{\mathrm{H_2O,aq}} + X_{\mathrm{NaCl,aq}}\right) \times \overline{V^{T,P_{\mathrm{sat}}}_{\mathrm{H_2O-NaCl}}} + X_{\mathrm{CH_4,aq}} \times \overline{V^{T,P}_{\mathrm{CH_4,aq}}} \quad (1)$$

where $X_{i,\mathrm{aq}}$ is the mole fraction of component i in the aqueous phase, $X_{\mathrm{CH_{4,aq}}}$ is calculated from the model of Duan et al. (1992a) at T, P and for a salinity m_{NaCl} (mole $\mathrm{kg^{-1}}$ H_2O) of the aqueous solution; $\overline{V^{T,P}_{\mathrm{aq},m_{\mathrm{NaCl}},m_{\mathrm{CH_4}}}}$ is the molar volume of the H_2O–NaCl–CH_4 aqueous solution, $\overline{V^{T,P_{\mathrm{sat}}}_{\mathrm{H_2O-NaCl}}}$ is the molar volume of H_2O–NaCl aqueous solution at temperature T and at saturation pressure (P_{sat}) with the same NaCl molality as the ternary fluid, $\overline{V^{T,P_{\mathrm{sat}}}_{\mathrm{H_2O-NaCl}}}$ is calculated from Haas (1976). $\overline{V^{T,P}_{\mathrm{CH_4,aq}}}$ is the partial molar volume of methane at infinite dilution in the aqueous phase for the P–T conditions; it is calculated from Duan et al. (1992a). The temperature chosen is the homogenisation temperature (T_{h}) and the pressure is calculated using the model of Duan et al. (1992a) by an iteration procedure on the pressure to obtain the methane concentration at T_{h} for the composition of the synthetic fluid inclusion (CH_4 and NaCl molalities).

Then, the density of the aqueous phase $\rho^{P,T}_{\mathrm{aq},m_{\mathrm{NaCl}},m_{\mathrm{CH_4}}}$ is calculated from Eq. (2):

$$\rho^{T,P}_{\mathrm{aq},m_{\mathrm{NaCl}},m_{\mathrm{CH_4}}} = \frac{\sum_{i=1}^{i=3} X_{i,\mathrm{aq}} \times \overline{M_i}}{\overline{V^{T,P}_{\mathrm{aq},m_{\mathrm{NaCl}},m_{\mathrm{CH_4}}}}} \quad (2)$$

where $X_{i,\mathrm{aq}}$ is the mole fraction of component i, m_i is the concentration of component i (molal), $\overline{M_i}$ is the molar mass of component i. At $T = T_{\mathrm{h}}$, the density of the aqueous phase is the bulk density: $\rho_{\mathrm{bulk}} = \rho^{T_{\mathrm{h}},P}_{\mathrm{aq},m_{\mathrm{NaCl}},m_{\mathrm{CH_4}}}$.

For any temperature T below the homogenisation, the volume fraction of the vapour phase, $f^{T,P}_{\mathrm{vap}}$, is calculated from Eq. (3) assuming constant density:

$$f^{T,P}_{\mathrm{vap}} = \frac{\rho_{\mathrm{bulk}} - \rho^{T,P}_{\mathrm{aq},m_{\mathrm{NaCl}},m_{\mathrm{CH_4}}}}{\dfrac{\overline{M_{\mathrm{CH_4}}}}{\overline{V^{T,P}_{\mathrm{vap,CH_4}}}} - \rho^{T,P}_{\mathrm{aq},m_{\mathrm{NaCl}},m_{\mathrm{CH_4}}}} \quad (3)$$

where $\overline{V^{T,P}_{\mathrm{vap,CH_4}}}$ is the molar volume of the vapour phase considered to be water-free as assumed in the model of Duan et al. (1992a) and calculated from the equation of state of Duan et al. (1992b). The density of the aqueous phase at temperature T, $\rho_{\mathrm{aq},m_{\mathrm{NaCl}},m^{T,P}_{\mathrm{CH_4}}}$, is calculated in the same manner as at T_{h}, but this requires the knowledge of the pressure, which is calculated by an iterative procedure explained below.

Eqs. (4)–(6) permit the calculation of the total number of moles of methane, $n^{T,P}_{\mathrm{CH_{4t}}}$, $n^{T,P}_{\mathrm{H_2O}}$, water, and $m^{T,P}_{\mathrm{CH_{4t}}}$ methane concentration at T and P in the molality scale:

$$n^{T,P}_{\mathrm{H_2O,t}} = \frac{100 - \mathrm{Wt\%_{NaCl}}}{100} \times \rho^{T,P}_{\mathrm{aq},m_{\mathrm{NaCl}},m_{\mathrm{CH_4}}} \times \left(1 - f^{T,P}_{\mathrm{vap}}\right) \quad (4)$$

$$n^{T,P}_{\mathrm{CH_4,t}} = \frac{f^{T,P}_{\mathrm{vap}}}{\overline{V^{T,P}_{\mathrm{vap,CH_4}}}} + m^{T,P,m_{\mathrm{NaCl}}}_{\mathrm{CH_4,aq}} \times \frac{n^{T,P}_{\mathrm{H_2O},t} \times \overline{M_{\mathrm{H_2O}}}}{1000} \quad (5)$$

$$m^{T,P}_{\mathrm{CH_4},t} = \frac{n^{T,P}_{\mathrm{CH_4},t} \times 1000}{n^{T,P}_{\mathrm{H_2O},t} \times \overline{M_{\mathrm{H_2O}}}} \quad (6)$$

A first estimation of pressure at temperature T is made and allows the calculation of $\overline{V^{T,P}_{\mathrm{aq},m_{\mathrm{NaCl}},m_{\mathrm{CH_4}}}}$ (Eq. 1), $\rho^{T,P}_{\mathrm{aq},m_{\mathrm{NaCl}},m_{\mathrm{CH_4}}}$ (Eq. 2), $f^{T,P}_{\mathrm{vap}}$ (Eq. 3) and $m^{T,P}_{\mathrm{CH_{4t}}}$ is obtained using Eqs. (4)–(6). If the calculated value of the methane concentration $m^{T,P,m_{\mathrm{NaCl}}}_{\mathrm{CH_4,aq}}$ differs from the known concentration of methane of the inclusion by less than $\varepsilon = 10^{-8}$, the calculation is stopped and the concentration of methane in the aqueous phase, $m^{T,P,m_{\mathrm{NaCl}}}_{\mathrm{CH_4,aq}}$ is assumed to be correct. It is worth noting that the pressure inside the fluid inclusion is also known and so it is possible to reconstruct the isochoric path of the fluid inclusion in the two phase field.

3.4. Calibration curves

The intensity ratios (CH_4 area/H_2O area) vs. the methane concentration of the aqueous solution is plotted for the stretching and bending of water for different temperatures (Fig. 4a and b, respectively).

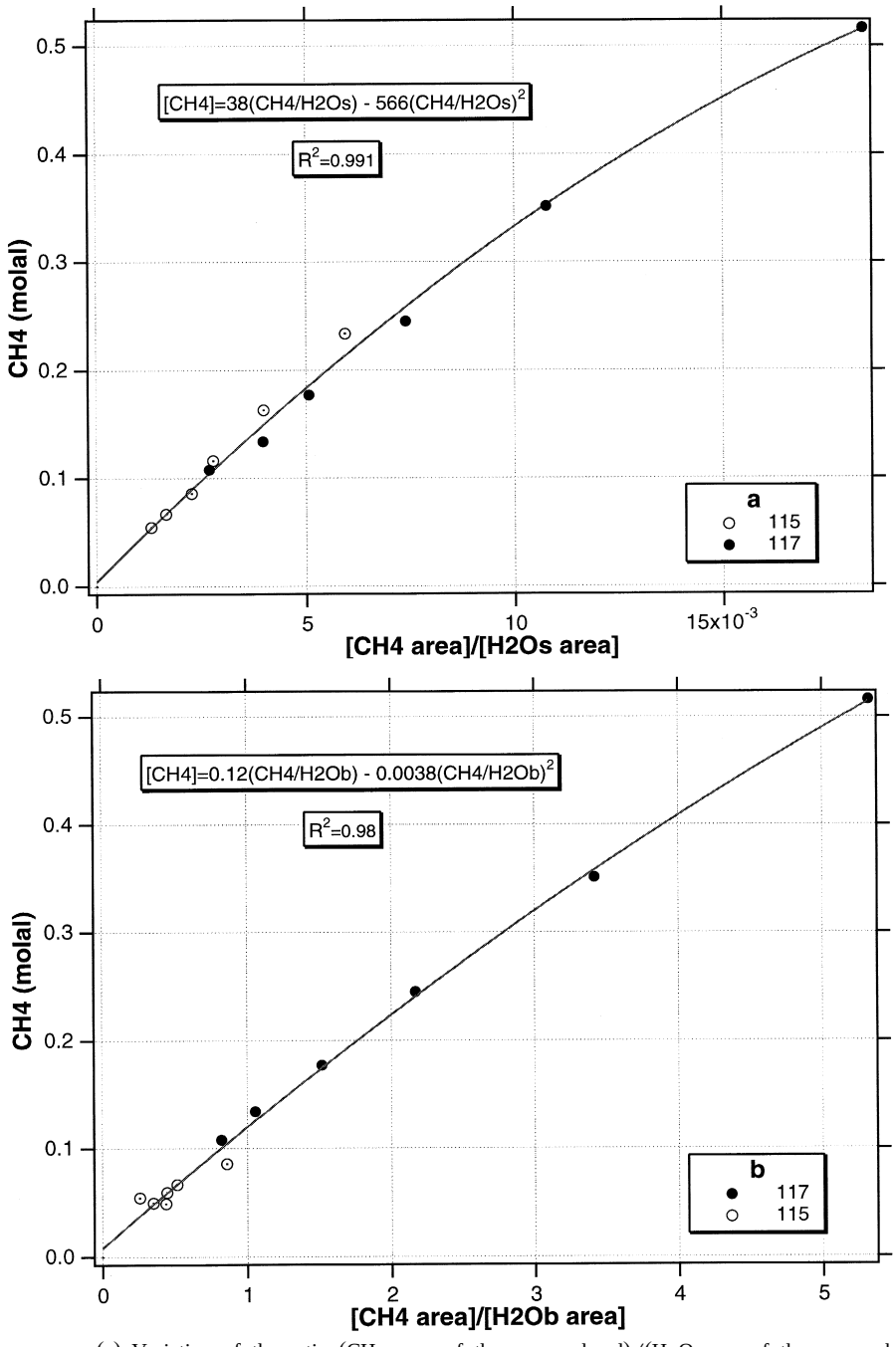

Fig. 4. Calibration curves. (a) Variation of the ratio (CH_4 area of the ν_{1,CH_4} band)/(H_2O area of the ν_{s,H_2O} band) vs. methane concentration (molality scale) for samples 117 and 115. (b) Variation of the ratio (CH_4 area of the ν_{1,CH_4} band)/(H_2O area of the ν_{b,H_2O} band) vs. methane concentration (molality scale) for samples 117 and 115.

High CH_4 concentrations correspond to high temperature measurements.

All the data are consistent within the experimental errors and are almost aligned along a straight line going through the origin. For analytical purposes, all data were reduced by a second-order polynomial regression. The accuracy for the determination of the methane concentration using this method is around 10%.

The calibration curve (Fig. 4b) based on the bending mode of water shows a linear distribution over the whole concentration range to 0.5 m CH_4. No temperature effect is identified. This shows that the bending mode may be a better choice for analytical purposes.

The bending mode is known to be less sensitive to hydrogen bonding and also to ion solvation compared to the stretching band of water (Ratcliffe and Irish, 1982). Thus, the intensity ratio is, as a first approximation, only a function of the concentration of methane. There is almost a linear trend for the stretching mode for medium concentrations, corresponding to temperatures up to 175°C. This suggests that the modification of the profile of the stretching band of water corresponds mainly to a modification of the distribution of OH oscillators between those involved in strong hydrogen bonding and those involved in weaker interaction, all these oscillators having similar Raman scattering cross-sections. At the highest concentrations corresponding to temperatures of 200–225°C, the thermal agitation produces a significant decrease in hydrogen bonding. The OH oscillators, less involved in hydrogen bonding, should have a smaller Raman scattering cross-section in order to explain the concave curvature of the calibration curve.

3.5. Isochore calculations in the single phase field

At the moment, no equation of state is available for calculating the isochore of a fluid inclusion above the homogenisation temperature in the CH_4–H_2O–NaCl system. Therefore, we propose the following method for aqueous-rich fluids with methane concentration below 1m NaCl concentration (m_{NaCl}) determined from microthermometry:

(1) determination of the methane concentration using Raman analysis a few degrees above the homogenisation temperature using the relevant calibration curve (T, m_{NaCl}), which must be extended to salt-bearing fluids;

(2) calculation of the fluid pressure (Pf_h) at the homogenisation temperature (T_h) using the thermodynamic model of Duan et al. (1992a): the pressure is calculated by an iterative procedure to reproduce the methane concentration, determined analytically, at T_h and for a fluid with a salinity, m_{NaCl};

(3) the isochore is drawn from the Pf_h–T_h point parallel to the isochore of a methane free fluid of the H_2O–NaCl system which has the same T_h and salinity (m_{NaCl}) as the methane-bearing fluid inclusions.

3.6. Application to natural samples

Raman analyses have been performed on aqueous inclusions from a sandstone oil reservoir of the mid-Jurassic Brent formation in the South Alwyn area of the North Sea basin. Diagenesis of the sandstone is characterised by quartz overgrowth and kaolinite cement dated between 60 and 45 Ma. This diagenetic episode is followed by illite precipitation between 50 and 40 Ma. Calcite precipitation can locally accompany quartz, kaolinite and illite. Petroleum migration took place at the end of diagenesis between 45 and 40 Ma in the East part of Alwyn South and between 40 to 35 Ma in the western part (Malley et al., 1986; Jourdan et al., 1987; Mogé and Pagel, 1990). This study has been focused on three specimens from three different wells (3/14a8 in the eastern part, 3/14b9 and 3/14a12 in the western part) located in the 3600–3700-m depth range and previously studied by Jourdan et al. (1987).

Diagenetic fluid inclusions are observed in fracture planes inside detrital quartz grains, in quartz overgrowth edges and rarely inside overgrowths. Aqueous two-phase (gas + liquid) inclusions are abundant and are sometimes associated with oil inclusions which are colourless and two-(gas + liquid) or three-phase (gas + liquid + black solid). FT-IR analyses show an aliphatic-dominated composition with the presence of methane and carbon dioxide. Microthermometric studies show complex behaviour at low temperature and homogenisation temperatures ranging from 82°C to 90°C (Fig. 5). No oil inclusion has been found in the sample from 3/14a12 well.

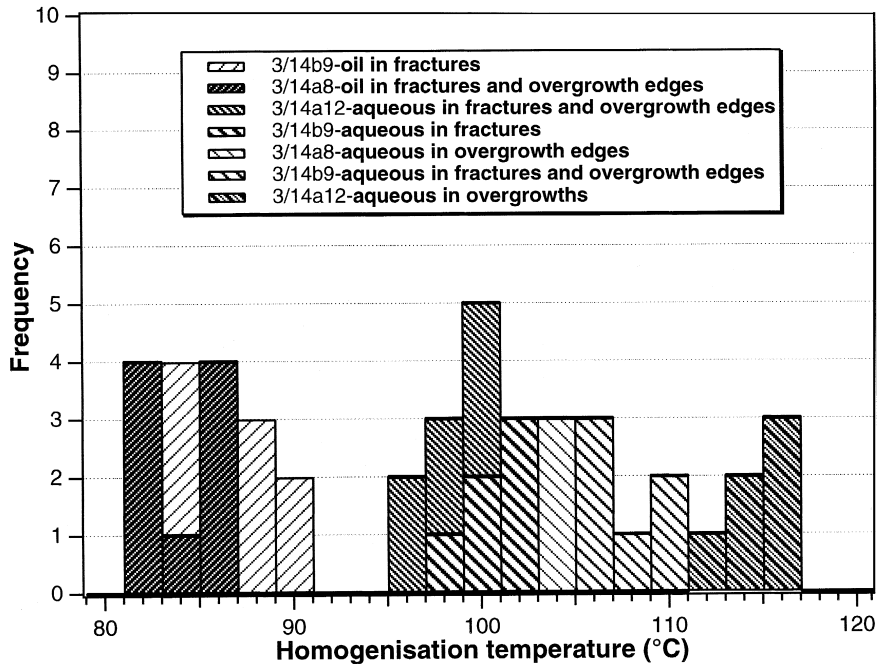

Fig. 5. Histograms of homogenisation temperatures of natural fluid inclusions.

Different aqueous inclusion populations, all homogenising to the liquid phase, have been characterised by their morphology, location and microthermometric behaviour. Type (1) inclusions exhibit a hexagonal shape in fracture planes inside detrital quartz grains with homogenisation temperatures

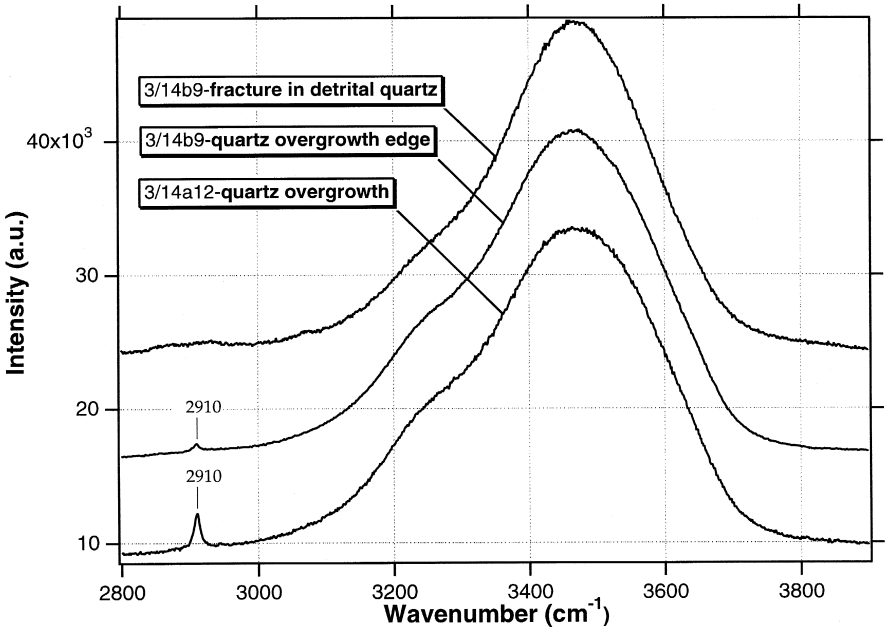

Fig. 6. Raman spectra obtained on three types of fluid inclusions a few degrees above the homogenisation temperature.

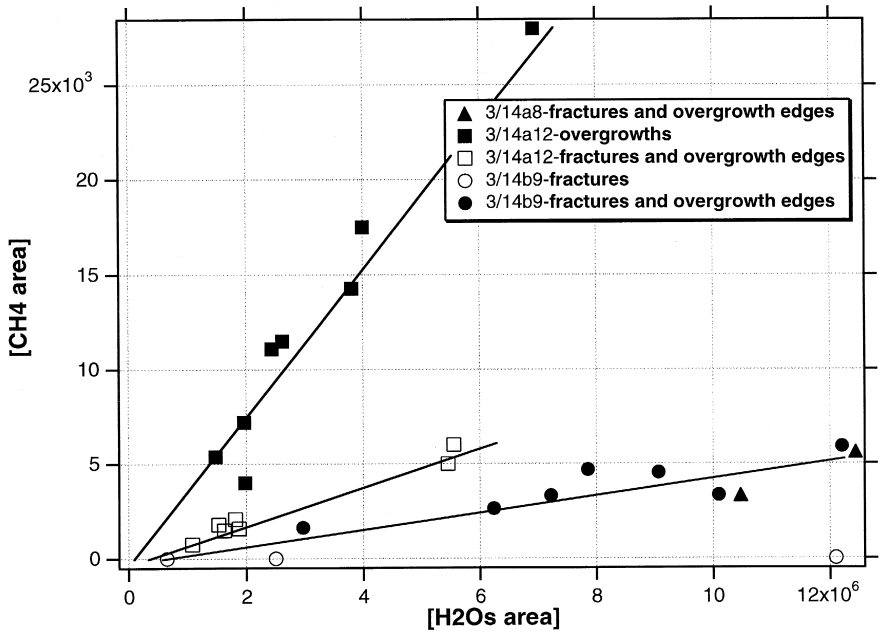

Fig. 7. Area of the Raman ν_{1,CH_4} band versus area of the Raman ν_{s,H_2O} band for the different types of fluid inclusions from Alwyn.

ranging from 98°C to 102°C. Type (2) inclusions have complex shapes in fracture planes inside quartz grains with homogenisation temperatures ranging from 98°C to 100°C (3/14a12 well) and from 104°C

Table 2
Alwyn South aqueous inclusion microthermometric and Raman data

Sample	Inclusion	Localisation	Shape	wt.% NaCl	T_h	$[CH_4]$(molal)
3/14a8	1	overg. edge	complex	1.2	101.8	0.017
-	2	-	-	1.0	103.1	0.012
3/14b9	3	fracture	hexagonal	2.5	98.5	0
-	4	-	-	2.4	100.7	0
-	5	-	-	1.1	99.1	0
-	6	fracture	complex	0.7	109.9	0.018
-	7	overg. edge	complex	0.4	107.1	0.017
-	8	-	-	0.2	108.6	0.021
-	9	-	-	1.2	105.6	0.016
-	10	-	-	0.5	106.0	0.022
-	11	-	-	0	110.1	0.019
3/14a12	12	overgrowth	irregular	0	110.9	0.158
-	13	-	-	0.7	114.7	0.144
-	14	-	-	0.6	113.8	0.134
-	15	-	-	0.2	115.3	0.131
-	16	-	-	0.3	116.1	0.132
-	17	-	-	0	112.0	0.075
-	18	fracture	complex	2.1	99.8	0.040
-	19	-	-	2.4	102.1	0.043
-	20	-	-	0.4	100.4	0.026
-	21	-	-	2.4	99.5	0.044
-	22	-	-	0	96.9	0.032
-	23	overg. edge	complex	0.6	98.2	0.035

to 110°C (3/14b9 well). Type (3) inclusions, with complex shape, are located at the quartz detrital-overgrowth boundary and have same T_h values as type 2 inclusions. Type (4) inclusions display irregular shapes and are inside quartz overgrowth and their homogenisation temperatures range between 112°C and 116°C.

The inclusions cannot be distinguished by salinity which is very low between 0 to 3 wt.% NaCl (≤ 0.5 m). This justifies the use of a pure water calibration curve for the calculation of methane concentrations in Alwyn inclusions. A histogram of homogenisation temperatures (Fig. 5) shows higher dispersion for aqueous than for oil inclusions. Raman spectra have been acquired a few degrees above the homogenisation temperature in homogeneous liquid inclusions (120°C). The methane stretching vibration is detected at 2910 cm^{-1} whatever type the inclusion is. It is similar for inclusions with complex shapes in fractures and quartz overgrowths but slightly different for hexagonal inclusions in fracture planes (Fig. 6).

The areas of the stretching vibrations of methane and water have been measured for each inclusion and are reported in Fig. 7. Methane concentration (Table 2) is deduced from the calibration curve previously established (Fig. 4a). Three inclusion populations can be distinguished by their characteristic CH_4/H_2Os area ratios: (1) inclusions in overgrowths with high CH_4/H_2Os ratios corresponding to 0.13–0.16 CH_4 molal concentrations (3/14a12 well), (2) inclusions in fractures and overgrowth edges with low CH_4/H_2Os ratio corresponding to

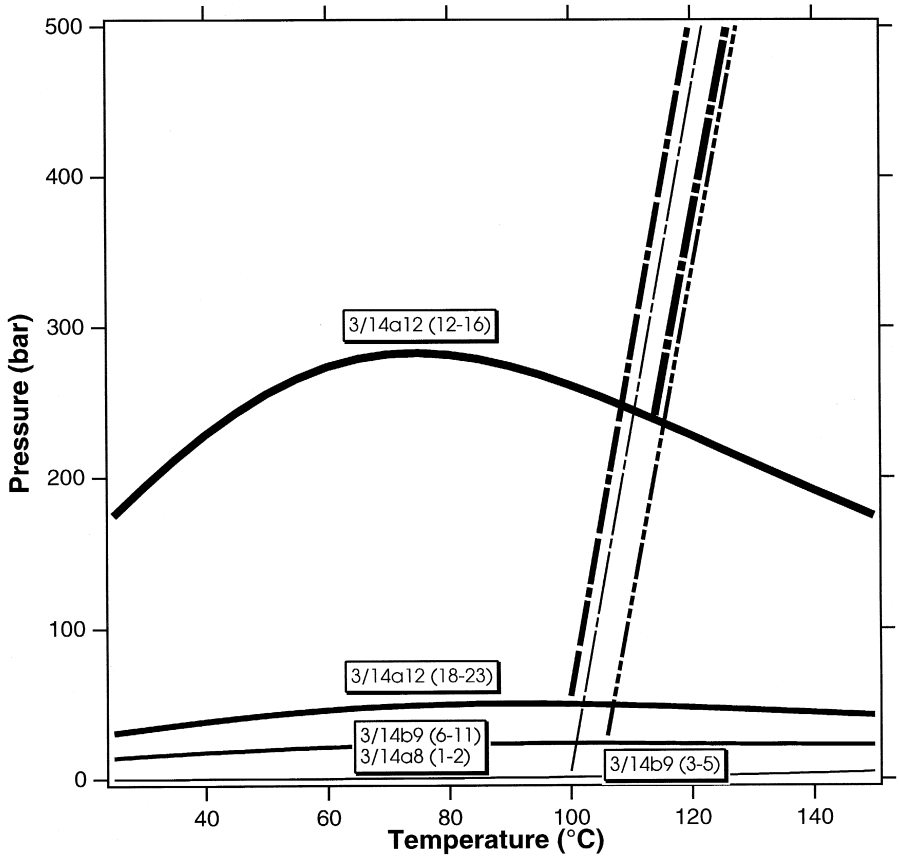

Fig. 8. P–T diagram for aqueous inclusions from Alwyn South area (North Sea basin). Isopleths and isochores have been drawn using the model of Duan et al. (1992a) for the isopleth and the equation Zhang and Frantz (1987) respectively. In parentheses : inclusion numbers corresponding to Table 2.

0.026–0.044 CH_4 molal concentrations (3/14a12) and to 0.012–0.022 CH_4 molal concentration (3/14a8 and 3/14b9 wells), and (3) inclusions with methane concentration below the detection limit (0.01m).

The bending vibration of water was not considered because of organic contamination in the form of oil impregnation along mineral boundaries and fracture planes or from the glue used for sample preparation: C=C and C=O vibrations can, partially mask the O-H bending vibration of water.

The average CH_4 molal concentration and T_h have been used to reconstruct isopleths and isochores in a P–T diagram (Fig. 8) following the Duan et al. equation of state (Duan et al., 1992b) for the different inclusion types and samples. Raman analyses allow the discrimination between aqueous inclusion populations with similar microthermometric behaviour. The methane concentration imposes severe constrains for pressure reconstruction. In the case of the Alwyn South environment, three main aqueous fluids have been detected. The methane-rich fluid is present to the end of the silicification diagenetic episode. The hypothesis of methane water saturation leads to trapping P–T conditions of 115°C and 240 bar equivalent to the temperature and pressure of homogenisation. This pressure estimate is consistent with hydrostatic pressure reconstruction at the time of oil migration (40–50 Ma), corresponding to about 2000 m of burial (Jourdan et al., 1987).

4. Conclusion

This study has demonstrated that it is possible to analyse methane at low concentrations ($0.01 < m_{CH_4} < 1$m) in aqueous-bearing fluid inclusions with a size (~ 10 μm) typical of the inclusions representative of diagenetic fluids found in sedimentary basins. First, calibration curves were established as a function of temperature using synthetic fluid inclusions heated from room temperature to a few degrees above the homogenisation temperature. Then the methane concentration in the aqueous phase co-existing with the vapour phase was determined from a computer program using the thermodynamic model of methane solubility in aqueous solution of Duan et al. (1992a). A procedure for the calculation of the isochore above the homogenisation temperature of aqueous-rich and methane-poor fluid inclusions has been proposed: it combines the Raman analysis of the methane content, the calculation of pressure at the homogenisation temperature and the isochoric properties of methane-free H_2O–NaCl fluid with the same salinity and T_h.

The first application of this technique to natural fluid inclusions from Alwyn area has been made. Three populations of aqueous fluid inclusions have been identified from their methane concentration, although microthermometric data could not discriminate between them. It is worth noting that these three types are not synchronous and that a relative chronology can be made. This progress in the analysis of the methane content at low concentrations (< 0.1m) exemplifies the variation in fluid chemistry during a short time interval of diagenesis. Further work is in progress to extend the calibration to salt-bearing solutions.

Acknowledgements

This work was supported by Elf and Total. The authors wish to thank F. Walgenwitz, F. Sommer, C. Demars, Robert Popp and C. Mc Shane for their helpful cooperation. R.C. Burruss, Z. Duan and an anonymous reviewer are kindly thanked for their constructive comments.

References

Bodnar, R.J., Bethke, P.M., 1984. Systematics of stretching of fluid inclusions: I. Fluorite and sphalerite at 1 atmosphere confining pressure. Econ. Geol. 79, 141–161.

Bodnar, R.J., Sterner, S.M., 1987. Synthetic fluid inclusions. In: Ulmer, G.C., Barnes, H.L. (Eds.), Hydrothermal Experimental Techniques. Wiley-Interscience, New York, pp. 423–457.

Deaton, W.M., Frost, E.M.Jr., 1948. Gas hydrate and their relation to the operation of natural gas pipe lines, U.S. Bur. Mines, Monogr. 8, 103 p.

Duan, Z., Moller, N., Greenberg, J.H., Weare, J.H., 1992a. The prediction of methane solubility in natural waters to high ionic strength from 0°C to 250°C and from 0 to 1600 bar. Geochim. Cosmochim. Acta 56, 1451–1460.

Duan, Z., Moller, N., Weare, J.H., 1992b. An equation of state (EOS) for CH_4,CO_2 and H_2O. Geochim. Cosmochim. Acta 56, 2605–2618.

Dubessy, J., Moissette, A., Bakker, R., Frantz, J.D., Zhang, Y.G.,

1998. High-temperature Raman spectroscopic study of H_2O–CO_2–CH_4 mixtures in synthetic fluid inclusions: first insights on molecular interactions and analytical implications. Eur. J. Mineral. 11, 23–32.

Frantz, J.D., Zhang, Y., Hickmott, D.D., Hoering, T.C., 1989. Hydrothermal reactions involving equilibrium between minerals and mixed volatiles: I. Techniques for experimentally loading and analyzing gases and their application to synthetic fluid inclusions. Chem. Geol. 76, 57–70.

Frantz, J.D., Dubessy, J., Mysen, B., 1993. An optical cell for Raman spectroscopic studies of supercritical fluids and its application to the study of water to 500°C and 2000 bars. Chem. Geol. 106, 9–26.

Gravier, J.F., 1986. Propriétés des fluides de gisements. Cours de production. Tome 2. Editions Technip. 262 p.

Haas, J.L.Jr., 1976. Physical properties of the coexisting phases and thermochemical properties of the H_2O component in boiling NaCl solution, Geological Survey Bulletin 1421-A. 73 p.

Herzberg, G., 1968. Molecular Spectra and Molecular Structure: II. Infrared and Raman spectra. Van Nostrand, London, 632 p.

Jourdan, A., Thomas, M., Brévart, O., Robson, P., Sommer, F., Sullivan, M., 1987. Diagenesis as the control of the Brent sandstone reservoir properties in the Greater Alwyn area (East Shetland Basin). In: Brooks, J., Glennie, K. (Eds.), Petroleum Geology of North West Europe. pp. 951–961.

Lamb, W.M., Popp, R.K., Boockoff, L.A., 1996. The determination of phase relations in the CH_4–H_2O–NaCl system at 1 bar, 400°C to 600°C using synthetic fluid inclusions. Geochim. Cosmochim. Acta, 1885–1897.

Malley, P., Jourdan, A., Weber, F., 1986. Etude des inclusions fluides dans les nourrissages siliceux des grès réservoirs de Mer du Nord: une nouvelle lecture possible de l'histoire diagénétique du Brent de la région d'Alwyn. C.R. Acad. Sc. Paris t. 302 (no 9), 653–658, Série II.

Mogé, M., Pagel, M., 1990. Petrography, fluid inclusion and stable isotopes of Jurassic carbonate-cemented sandstones (Viking graben-North Sea). Chem. Geol. 84, 243–245.

Price, L.C., 1981. Aqueous solubility of crude oil to 400°C and 200 bars pressure in the presence of gas. J. Pet. Geol. 4, 195–223.

Ratcliffe, C.I., Irish, D.E., 1982. Vibrational studies of solution at elevated temperatures and pressures, 5. Raman studies of liquid water up to 300°C. J. Phys. Chem. 86, 4897–4905.

Rull, F., Alvarez, J., Edwards, H.G.M., 1996. Program for data analysis in Raman spectroscopy. GeoRaman, Toulouse.

Sterner, S.M., Bodnar, R.J., 1984. Synthetic fluid inclusions in natural quartz: I. Compositional types synthesized and applications to experimental geochemistry. Geochim. Cosmochim. Acta 48, 2659–2668.

Wilkins, R.W.T., 1986. The mechanisms of stretching and leaking of fluid inclusions in fluorite. Econ. Geol. 81, 1003–1008.

Zhang, Y.G., Frantz, J.D., 1987. Determination of the homogenisation temperatures and densities of supercritical fluids in the system NaCl–KCl–$CaCl_2$–H_2O using synthetic fluid inclusions. Chem. Geol. 64, 335–350.